Journal of Alloys and Compounds 509 (2011) 3257–3261

Contents lists available at ScienceDirect

Journal of Alloys and Compounds

journal homepage: www.elsevier.com/locate/jallcom

Combustion synthesis of vanadium borides

C.L. Yeh*, H.J. Wang

Department of Aerospace and Systems Engineering, Feng Chia University, 100 Wenhwa Rd., Seatwen, Taichung 40724, Taiwan

ARTICLE INFO

Article history:
Received 8 October 2010
Received in revised form
26 November 2010
Accepted 1 December 2010
Available online 8 December 2010

Keywords:
Transition metal compounds
Solid state reactions
X-ray diffraction
Vanadium boride
Combustion synthesis

ABSTRACT

An experimental study on the preparation of various vanadium borides (including V_3B_2, VB, V_5B_6, V_3B_4, V_2B_3, and VB_2) in the V–B system was conducted by self-propagating high-temperature synthesis (SHS) from the elemental powder compacts. Close flame-front velocities and comparable combustion temperatures were observed for the reactant compacts with V:B = 1:1, 5:6, and 3:4, and they were much higher than those for the samples of other compositions. The lowest combustion velocity and temperature were detected in the sample of V:B = 1:2. According to the XRD analysis, pure VB was produced not only from the sample of V:B = 1:1, but also from those of V:B = 5:6 and 3:4. For the powder compact with V:B = 1:2, VB_2 was dominantly formed along with trivial amounts of VB and V_3B_4. A multiphase product composed of VB and V_3B_4 at comparable quantities was yielded from the sample of V:B = 2:3. The only V-rich sample formulated at V:B = 3:2 generated monoboride VB and left the end product a large amount of unreacted vanadium.

1. Introduction

Borides of the transition metals of groups IVB and VB, such as TiB_2, ZrB_2, VB_2, and TaB_2, are known as ultra high-temperature ceramics. Besides high melting temperatures, they have a unique combination of high hardness, high electrical and thermal conductivity, good chemical stability, good wear resistance, and excellent corrosion resistance [1–6]. Of particular interest for this study are the borides of vanadium. According to the V–B phase diagram [7], there are six boride phases including V_3B_2, VB, V_5B_6, V_3B_4, V_2B_3, and VB_2. In addition to as surface protection components and wear resistant materials, vanadium borides are promising for use as the anode material for alkaline batteries due to their exceptionally high discharge capacity [8–10].

Preparation of vanadium borides has been implemented by a variety of processing routes, including the direct combination of elemental vanadium with boron in a high-energy shaker ball-miller [10] or a triarc furnace [11], borothermic reduction of vanadium oxide (V_2O_3) [12], and solid state reaction between vanadium chloride and MgB_2, $NaBH_4$, or $LiBH_4$ [13–15]. As a promising alternative, combustion synthesis in the self-propagating high-temperature synthesis (SHS) mode takes advantage of the self-sustaining merit from highly exothermic reactions, and hence, has the potentials of low energy requirement, short reaction time, and simple facilities [16–19]. Formation of transition metal borides by the SHS technique is typically through the direct reaction of mixed constituent elements in a sample compact, by which numerous borides like TiB_2, TiB, ZrB_2, HfB_2, NbB_2, NbB, TaB_2 and TaB have been synthesized [16,20–25]. When direct combustion between the metal and boron is not feasible, the SHS process involving borothermic reduction of a metal oxide has been adopted. For example, borides of chromium (Cr_5B_3, CrB, and CrB_2) and molybdenum (Mo_2B, MoB_2, and Mo_2B_5) were produced from the reduction of Cr_2O_3 and MoO_3, respectively, by amorphous boron [26,27].

Despite the fact that many transition metal borides have been produced by combustion synthesis, few studies have been performed on the preparation of vanadium borides by SHS. Therefore, this study aims to explore the feasibility of producing various vanadium borides by the SHS process using elemental powder compacts of their corresponding stoichiometries. Effects of the starting composition and temperature of the reactant compact were studied on the combustion temperature, flame-front velocity, and sustainability of the synthesis reaction. The phase constituent of the final product was identified by XRD. In addition, the apparent activation energy associated with formation of the specific boride phase was determined by correlating the dependence of flame-front velocity on combustion temperature.

2. Experimental methods of approach

Vanadium (Aldrich, <45 μm, 99.5% purity) and amorphous boron (Noah Technologies Corp., 1 μm, 92% purity) powders were used as the starting materials in this study. Powder blends with six different molar ratios including V:B = 3:2, 1:1, 5:6, 3:4, 2:3, and 1:2 were prepared in a ball mill. In order to obtain homogeneous powder mixtures, a cylindrical capped container was partially filled with the reactant powders and several ceramic balls (5 mm in diameter). The container sat on

* Corresponding author. Tel.: +886 4 24517250x3963; fax: +886 4 24510862.
E-mail address: clyeh@fcu.edu.tw (C.L. Yeh).

0925-8388/$ – see front matter © 2010 Elsevier B.V. All rights reserved.
doi:10.1016/j.jallcom.2010.12.004

two drive shafts, one of which rotated around a horizontal axis, in the ball mill and the powders were dry mixed at 120 rpm for 10 h. Mixed powders were then cold-pressed into the cylindrical sample compact with a diameter of 7 mm, a height of 12 mm, and a compaction density relative to 50% of the theoretical maximum density (TMD).

The SHS experiments were conducted in a stainless-steel windowed combustion chamber under an atmosphere of high purity argon (99.99%). The sample holder was equipped with a 600 W cartridge heater used to raise the initial temperature of the reactant compact prior to ignition. Moreover, a compressed pellet made up of Ti and carbon powders with Ti:C = 1:1 was placed on the top of the sample to serve as an ignition enhancer which was triggered by a heated tungsten coil. Details of the experimental setup and measurement approach were reported elsewhere [28]. The phase constituent of the synthesized product was identified by an X-ray diffractometer (Shimadzu XRD-6000) with Cu K_α radiation.

3. Results and discussion

3.1. Observation of combustion characteristics

Fig. 1(a)–(c) presents three typical SHS sequences illustrating solid state combustion of the V–B powder compacts with different initial compositions and temperatures. As shown in Fig. 1(a),

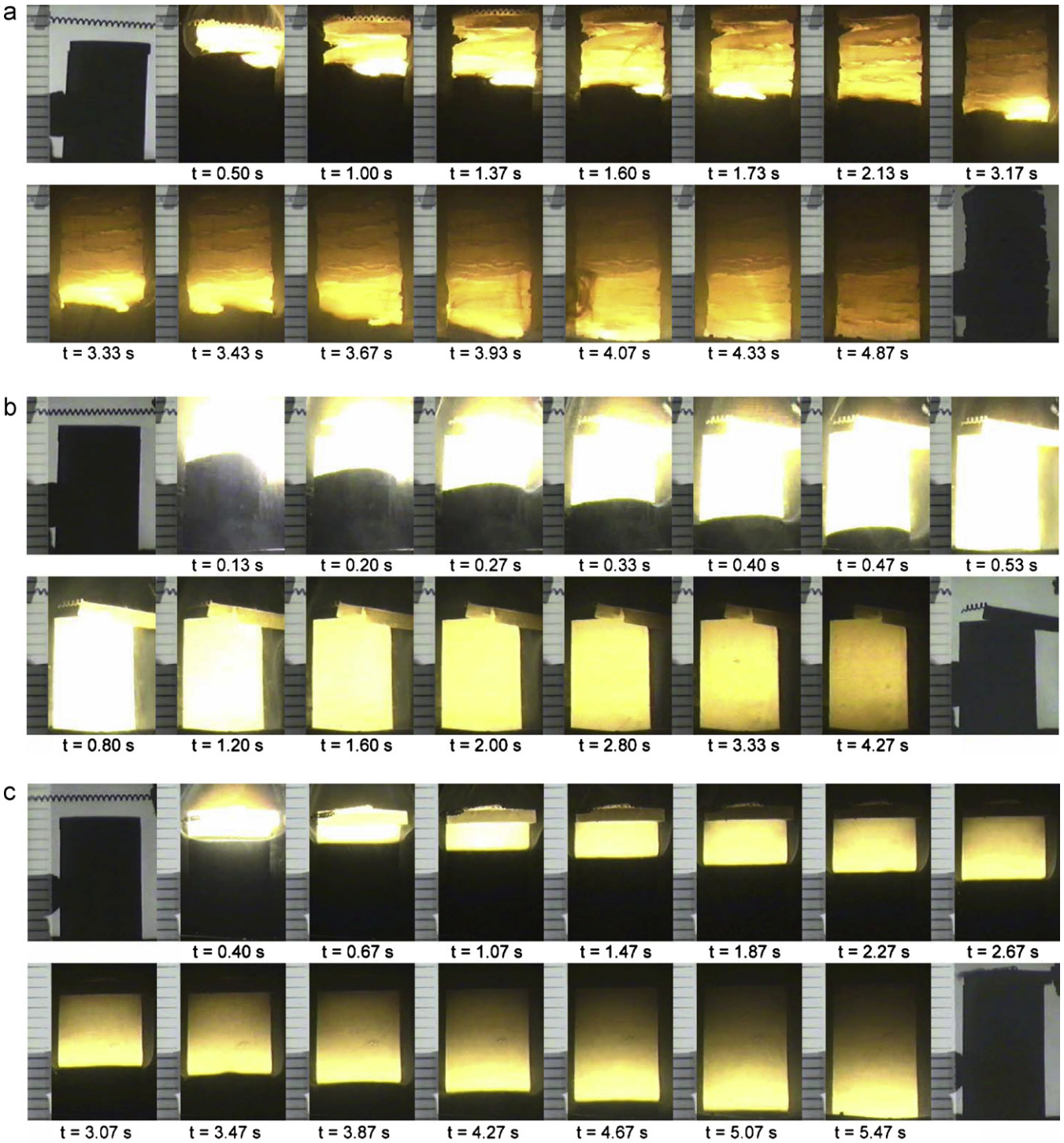

Fig. 1. Typical SHS sequences recorded from V–B powder compacts with different molar ratios and preheating temperatures: (a) V:B = 5:6 and without prior heating, (b) V:B = 1:1 and T_p = 300 °C, and (c) V:B = 1:2 and T_p = 300 °C.

the combustion of a sample composed of V:B = 5:6 under no prior heating was confined to a localized reaction zone propagating along a spiral trajectory. Self-sustaining combustion featuring a spinning reaction wave rather than a planar flame front is considered as an unstable combustion phenomenon and is mainly caused by the lack of sufficient heat flux generated from the reaction [29,30]. The spinning combustion wave not only prolonged the propagation time, but also caused significant delamination of the final product.

Experimental evidence indicated that except for the powder compact with V:B = 1:2, the SHS processes of other samples under no prior heating or preheating at 100 °C were subjected to the spinning combustion mode. Steady propagation of a planar front was achieved when the preheating temperature (T_p) was raised to 200 and 300 °C. As displayed in Fig. 1(b), for the sample of V:B = 1:1 at T_p = 300 °C, a distinct combustion front forms upon ignition and rapidly traverses the entire sample in about 0.53 s.

When the sample of V:B = 1:2 was employed, however, combustion ceased to propagate after initiation and quenched even in the case of T_p = 200 °C. With further increase in the preheating temperature to 300 °C, self-sustaining combustion characterized by a planar but slow reaction front was attained. Fig. 1(c) indicates that it takes as long as 5.47 s for the combustion front to arrive at the bottom of the sample, which implies that the reaction exothermicity related to this stoichiometry is substantially weaker in comparison to the others.

3.2. Measurement of flame-front velocity and combustion temperature

Based upon the recorded combustion images, the propagation velocity (V_f) of the steady combustion front was determined. Fig. 2 plots the flame-front velocities of six different samples under two preheating temperatures of 200 and 300 °C. An increase in the preheating temperature led to a higher spreading rate of the reaction front. Moreover, with the increase of the content of boron in the sample from 40 to 50 at.%, Fig. 2 shows a significant increase in the flame-front velocity approximately from 9.1 to 20.1 mm/s for T_p = 300 °C and 4.4 to 12.7 mm/s for T_p = 200 °C. However, the flame velocities of the reactant compacts with V:B = 1:1, 5:6, and 3:4 were comparable, due probably to their close stoichiometries. Further increase of boron caused a noticeable decrease in the reaction front velocity. Consequently, the slowest combustion wave with a propagation rate of 2.1 mm/s was observed in the sample containing the highest percent of boron (i.e., 66.7 at.% or V:B = 1:2) at T_p = 300 °C. It should be noted that at T_p = 200 °C, the lowest velocity of 3.2 mm/s was measured from the sample with 60 at.% of boron (i.e., V:B = 2:3), because of no reaction for the sample of V:B = 1:2.

The composition dependence of the combustion velocity is most likely attributed to the variation of reaction exothermicity with the powder compacts of different stoichiometries. Fig. 3 depicts six combustion temperature profiles recorded from combustion of different powder compacts at T_p = 300 °C. The abrupt rise in the temperature curve signifies the rapid arrival of the combustion wave and the peak value corresponds to the reaction front temperature. As revealed in Fig. 3, the peak temperature varies between 1262 and 1620 °C. The combustion temperature is essentially affected by the heat of formation and specific heat of the product. Close combustion temperatures observed for the powder compacts with V:B = 1:1, 5:6, and 3:4 are mainly attributed to the production of the same boride, VB, from these three samples.

When compared to those of the powder compacts with V:B = 1:1, 5:6, and 3:4, the lower combustion temperature for the sample of V:B = 2:3 is due to the formation of VB and V_3B_4 in the final product. Though the heat of formation of V_3B_4 is larger than that of VB [33,34], the specific heat of V_3B_4 is much higher than that of VB [34]. The lowest combustion front temperature observed in the sample

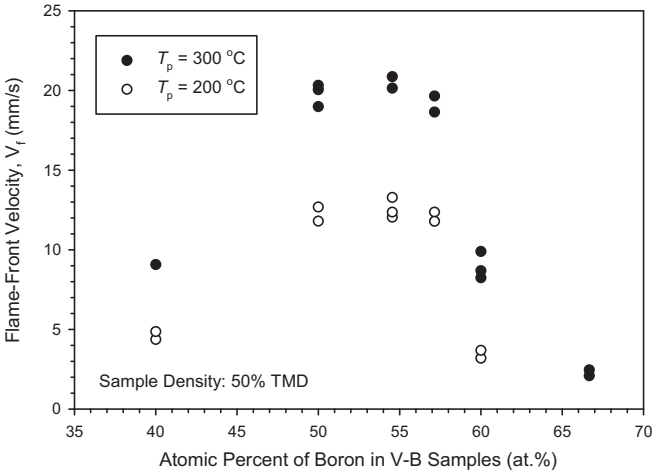

Fig. 2. Effects of starting stoichiometry and preheating temperature on flame-front propagation velocity of V–B powder compacts.

of V:B = 1:2 is a consequence of the formation of VB_2 as the dominant boride. The heat of formation of VB_2 is only slightly lower than those of VB, V_5B_6, V_3B_4 and V_2B_3. At temperatures of 1000–2000 K, however, the specific heat of VB_2 is about 25% higher than that of VB [34]. Most importantly, the composition dependence of the combustion front temperature is consistent with that of the flame-front velocity. This confirms the responsibility of reaction exothermicity for the combustion wave velocity.

Moreover, because the layer-by-layer heat transfer from the combustion front to the green sample plays a critical role in the SHS process, the combustion front velocity depends not only on the combustion temperature but also on the specific heat of the reactant powders. The specific heat of elemental boron is about twice larger than that of vanadium at 298 K [34]. This means that the sample with a higher content of boron requires more energy to raise its temperature to the ignition temperature. This further explains the considerably low flame velocity for the sample of V:B = 1:2, which represents the most boron-rich composition.

3.3. Phase constituents of combustion products

Based upon the XRD analysis, it was found that the boride phase formed from solid state combustion of the V-rich sample with V:B = 3:2 was monoboride VB, besides which a large amount of elemental vanadium left unreacted was detected. This means

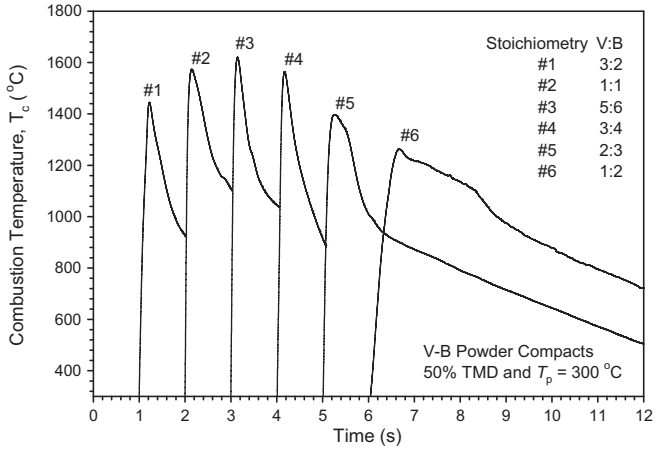

Fig. 3. Effect of starting stoichiometry on combustion temperature of V–B powder compacts with a preheating temperature of 300 °C.

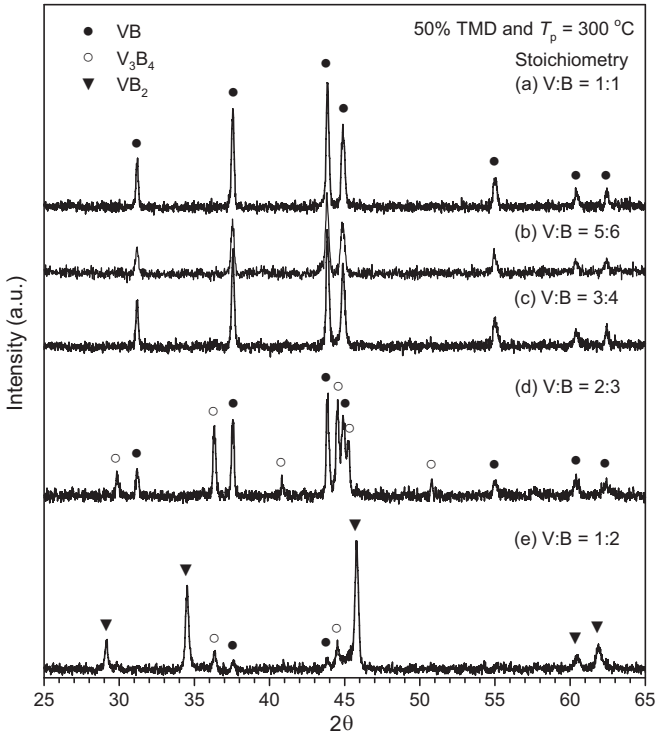

Fig. 4. XRD patterns of final products synthesized from powder compacts with (a) V:B = 1:1, (b) V:B = 5:6, (c) V:B = 3:4, (d) V:B = 2:3, and (e) V:B = 1:2.

an incomplete phase conversion. For the powder compacts of V:B = 1:1, 5:6, and 3:4, as shown in Fig. 4(a)–(c), single-phase VB was produced. This also explains the comparable combustion temperatures and similar flame-front velocities observed for the samples of these three compositions. The XRD pattern of the final product obtained from the sample of V:B = 2:3 is plotted in Fig. 4(d), revealing the yield of two boride phases VB and V_3B_4. For the resulting product from the sample of V:B = 1:2, Fig. 4(e) shows the formation of VB_2 as the dominant boride along with VB and V_3B_4 as the trivial phases. Among six vanadium borides, it is found that VB and VB_2 are the two borides produced in a pure or nearly pure form. On the contrary, some boride phases, like V_3B_2, V_5B_6, and V_2B_3, did not appear in any end products. This might suggest that they are kinetically unfavorable phases to be formed through solid state combustion of their constituent elements. Besides, the absence of V_3B_2, V_5B_6 and V_2B_3 is caused probably by the reason that the crystal structure of these compounds is too complicated to form during the SHS process subjected to a fast cooling rate.

3.4. Determination of activation energy

In view of the formation of single-phase VB from the powder compact of V:B = 1:1, it is highly instructive to deduce the activation energy for combustion synthesis of VB on the basis of the measured flame-front velocity and combustion temperature. The apparent activation energy of the solid state reaction is generally determined by realizing the dependence of the reaction front velocity on combustion temperature. Such a relationship has been expressed in the following simplified form [31,32].

$$\left(\frac{V_f}{T_c}\right)^2 = f(n)\left(\frac{R}{E_a}\right) K \exp\left(-\frac{E_a}{RT_c}\right) \quad (1)$$

where V_f is the flame-front propagation velocity, T_c the combustion front temperature, E_a the activation energy of the reaction, R the universal gas constant, $f(n)$ a function of the kinetic order of the reaction, and K a constant which accounts for the heat capacity of the product, the thermal conductivity, and the heat of reaction. According to Eq. (1), the slope of a straight line correlating $\ln(V_f/T_c)^2$ versus $1/T_c$ can provide the apparent activation energy of the reaction.

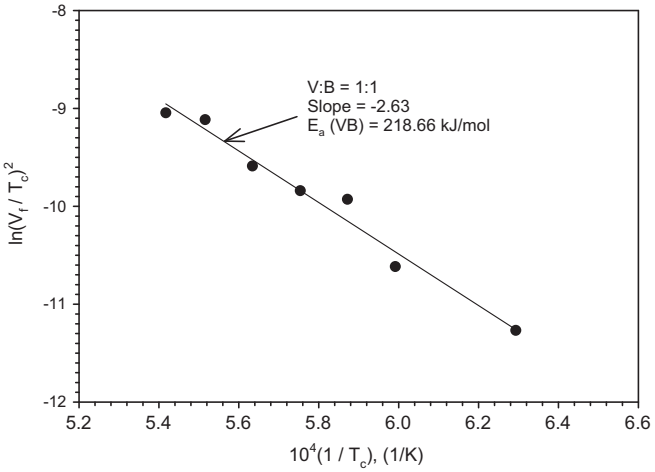

Fig. 5. Relation between flame-front velocity and combustion temperature for determination of activation energy of formation VB by combustion synthesis.

The relative change in the reaction front velocity with respect to combustion temperature can be established by diluting the reactant compact with an inert compound. As suggested by Bertolino et al. [32], the boride VB synthesized in this study is the most suitable candidate as the diluent for the powder mixture of V:B = 1:1. Intentionally, the mole fraction of VB as a diluent in the powder mixture was ranged from 2 to 10%. With the increase of the extent of dilution, the flame-front velocity decreased from 20.1 mm/s for the undiluted sample at T_p = 300 °C to 5.68 mm/s for the 10 mol% VB-diluted compact preheated at the same temperature. The combustion front temperature (T_c) decreased correspondingly from 1573 to 1316 °C. Fig. 5 plots the data of $\ln(V_f/T_c)^2$ versus $1/T_c$ and a best-fitted correlation line, from which the apparent activation energy of 218.66 kJ/mol is determined for combustion synthesis of VB. Due to weak exothermicity of the reaction, however, the above method was not applicable for the sample with V:B = 1:2.

4. Conclusions

This study represents the first attempt to investigate the feasibility of producing specific vanadium borides (including V_3B_2, VB, V_5B_6, V_3B_4, V_2B_3, and VB_2) from elemental powder compacts of their corresponding stoichiometries by combustion synthesis in the SHS mode. A preheating temperature (T_p) of 200 °C was required for all V-B reactant compacts, except 300 °C for the sample of V:B = 1:2, to achieve stable combustion featuring a planar reaction front. Otherwise, combustion was confined to a spinning reaction zone or was extinguished.

Among six different samples, the powder compacts of V:B = 1:1, 5:6, and 3:4 showed relatively high and comparable combustion propagation rates ranging between 18.6 and 20.9 mm/s at T_p = 300 °C. For the samples of V:B = 3:2 and 2:3 at T_p = 300 °C, the flame-front velocities were just about 8.5–10 mm/s. The lowest combustion velocity of 2.1 mm/s was observed in the sample of V:B = 1:2. The combustion front temperature varied from 1262 to 1620 °C and the composition dependence of the combustion temperature was in a manner consistent with that of the reaction front velocity.

Based upon the XRD analysis, VB and VB_2 were the only two borides produced almost monolithically from the powder com-

pacts of their equivalent compositions. Moreover, pure VB was obtained not only from the sample of V:B = 1:1, but also from those with V:B = 5:6 and 3:4. The resulting product of the sample with V:B = 3:2 contained VB and some remnant vanadium, implying an incomplete phase conversion. For the sample with V:B = 2:3, both VB and V_3B_4 was formed in the end product. In addition, the apparent activation energy deduced for combustion synthesis of VB was 218.66 kJ/mol.

Acknowledgements

This research was sponsored by the National Science Council of Taiwan, ROC, under the grants of NSC 98-2221-E-035-065-MY2.

References

[1] R.G. Munro, Material properties of titanium diboride, J. Res. Natl. Inst. Stand. Technol. 105 (2000) 709–720.
[2] W.G. Fahrenholtz, G.E. Hilmas, I.G. Talmy, J.A. Zaykoski, Refractory diborides of zirconium and hafnium, J. Am. Ceram. Soc. 90 (5) (2007) 1347–1364.
[3] S.Q. Guo, Densification of ZrB_2-based composites and their mechanical and physical properties: a review, J. Eur. Ceram. Soc. 29 (2009) 995–1011.
[4] X. Zhou, H. Zhang, C. Cheng, J. Gao, G. Xu, Y. Li, Y. Luo, First-principles study of structural, electronic and elastic properties of diboride of vanadium, Physica B 404 (2009) 1527–1531.
[5] X. Zhang, G.E. Hilmas, W.G. Fahrenholtz, Synthesis, densification, and mechanical properties of TaB_2, Mater. Lett. 62 (2008) 4251–4253.
[6] G.E. Grechnev, A.V. Fedorchenko, A.V. Logosha, A.S. Panfilov, I.V. Svechkarev, V.B. Filippov, A.B. Lyashchenko, A.V. Evdokimova, Electronic structure and magnetic properties of transition metal diborides, J. Alloys Compd. 481 (2009) 75–80.
[7] T.B. Massalski, H. Okamoto, P.R. Subramanian, L. Kacprzak (Eds.), Binary Alloy Phase Diagrams, ASM International Materials Park, OH, USA, 1996.
[8] X. Yu, S. Licht, A novel high capacity, environmentally benign energy storage system: super-ion boride battery, J. Power Sources 179 (2008) 407–411.
[9] H.X. Yang, Y.D. Wang, X.P. Ai, C.S. Cha, Metal borides: competitive high capacity anode materials for aqueous primary batteries, Electrochem. Solid-State Lett. 7 (2004) A212–A215.
[10] Y. Wang, X.Y. Guang, Y.L. Cao, X.P. Ai, H.X. Yang, Mechanochemical synthesis and electrochemical characterization of VB_x as high capacity anode materials for batteries, J. Alloys Compd. 501 (2010) L12–L14.
[11] C. Bulfon, A. Leithe-Jasper, H. Sassik, P. Rogl, Microhardness of Czochralski-grown single crystals of VB_2, J. Solid State Chem. 133 (1997) 113–116.
[12] P. Peshev, L. Leyarovska, G. Bliznakov, On the borothermic preparation of some vanadium, niobium, and tantalum borides, J. Less Common Met. 15 (1968) 259–267.
[13] L. Rao, E.G. Gillan, R.B. Kaner, Rapid synthesis of transition-metal borides by solid-state metathesis, J. Mater. Res. 10 (1995) 353–361.
[14] L. Shi, Y. Gu, L. Chen, Z. Yang, J. Ma, Y. Qian, Low-temperature synthesis of nanocrystalline vanadium diboride, Mater. Lett. 58 (2004) 2890–2892.
[15] J.W. Kim, J.H. Shim, J.P. Ahn, Y.W. Cho, J.H. Kim, K.H. Oh, Mechanochemical synthesis and characterization of TiB_2 and VB_2 nanopowders, Mater. Lett. 62 (2008) 2461–2462.
[16] A.G. Merzhanov, Combustion processes that synthesize materials, J. Mater. Process. Technol. 56 (1996) 222–241.
[17] Z.A. Munir, U. Anselmi-Tamburini, Self-propagating exothermic reactions: the synthesis of high-temperature materials by combustion, Mater. Sci. Rep. 3 (1989) 277–365.
[18] C.L. Yeh, in: K.H.J. Buschow, R.W. Cahn, M.C. Flemings, E.J. Kramer, S. Mahajan, P. Veyssiere (Eds.), Encyclopaedia of Materials: Science and Technology, Elsevier, Amsterdam, 2010.
[19] C.L. Yeh, in: M. Lackner (Ed.), Combustion Synthesis – Novel Routes to Novel Materials, Bentham Science, 2010.
[20] A.G. Merzhanov, I.P. Borovinskaya, Self-propagated high-temperature synthesis of refractory inorganic compounds, Dokl. Akad. Nauk USSR 204 (1972) 366–369.
[21] J.B. Holt, D.D. Kingman, G.M. Bianchini, Kinetics of the combustion synthesis of TiB_2, Mater. Sci. Eng. 71 (1985) 321–327.
[22] D.D. Radev, M. Marinov, Properties of titanium and zirconium diborides obtained by self-propagated high-temperature synthesis, J. Alloys Compd. 244 (1996) 48–51.
[23] J. Wong, E.M. Larson, P.A. Waide, R. Frahm, Combustion front dynamics in the combustion synthesis of refractory metal carbides and diborides using time-resolved X-ray diffraction, J. Synchrotron Radiat. 13 (2006) 326–335.
[24] H.E. Camurlu, F. Maglia, Preparation of nano-size ZrB_2 by self-propagating high-temperature synthesis, J. Eur. Ceram. Soc. 29 (2009) 1501–1506.
[25] C.L. Yeh, W.H. Chen, A comparative study on combustion synthesis of Nb–B compounds, J. Alloys Compd. 422 (2006) 78–85.
[26] C.L. Yeh, H.J. Wang, Preparation of borides in Nb–B and Cr–B systems by combustion synthesis involving borothermic reduction of Nb_2O_5 and Cr_2O_3, J. Alloys Compd. 490 (2010) 366–371.
[27] C.L. Yeh, W.S. Hsu, Preparation of molybdenum borides by combustion synthesis involving solid-phase displacement reactions, J. Alloys Compd. 457 (2008) 191–197.
[28] C.L. Yeh, Y.L. Chen, An experimental study on self-propagating high-temperature synthesis in the Ta–B_4C System, J. Alloys Compd. 478 (2009) 163–167.
[29] A.G. Merzhanov, Solid flames: discoveries, concepts, and horizons of cognition, Combust. Sci. Technol. 98 (1994) 307–336.
[30] T.P. Ivleva, A.G. Merzhanov, Three-dimensional spinning waves in the case of gas-free combustion, Dokl. Phys. 45 (2000) 136–141.
[31] C.L. Yeh, W.H. Chen, Preparation of niobium borides NbB and NbB_2 by self-propagating combustion synthesis, J. Alloys Compd. 420 (2006) 111–116.
[32] N. Bertolino, U. Anselmi-Tamburini, F. Maglia, G. Spinolo, Z.A. Munir, Combustion synthesis of Zr–Si intermetallic compounds, J. Alloys Compd. 288 (1999) 238–248.
[33] K.E. Spear, J.H. Blanks, M.S. Wang, Thermodynamic modeling of the V–B system, J. Less Common Met. 82 (1981) 237–243.
[34] M. Binnewies, E. Milke, Thermochemical Data of Elements and Compounds, Wiley-VCH Verlag GmbH, Weinheim, New York, 2002.